國 立 交 通 大 學

電子物理研究所

碩士論文

氧硒化鋅等電性半導體
之光激螢光時間解析研究

Time-resolved photoluminescence of isoelectronic $ZnSe_{1-x}O_x$ semiconductors

研究生：鍾蕙璘

指導教授：周武清 教授

中華民國九十九年五月

氧硒化鋅等電性半導體之光激螢光時間解析研究

Time-resolved photoluminescence of isoelectronic $ZnSe_{1-x}O_x$ semiconductors

研 究 生：鍾蕙璘　　Student：Hui-Lin Chung

指導教授：周武清 教授　　Advisor：Prof. Wu-Ching Chou

國 立 交 通 大 學

電子物理研究所

碩 士 論 文

A Thesis
Submitted to Institute of Electrophysics
College of Science
National Chiao Tung University
in partial Fulfillment of the Requirements
for the Degree of Master
in
Electrophysics
May 2010
Hsinchu, Taiwan, Republic of China

中華民國九十九年五月

氧硒化鋅等電性半導體
之光激螢光時間解析研究

研究生：鍾蕙璘　　指導教授：周武清 教授

國立交通大學電子物理研究所

中文摘要

在摻雜氧的硒化鋅中，氧會形成等電性中心並抓住載子，這將使載子的復合路徑變得複雜。在本研究中，我們使用光激螢光光譜與時間解析光譜來探討氧對載子復合機制的影響 (氧硒化鋅的氧含量最高為5.3莫耳百分比) 。我們發現氧除了會造成很大的能帶彎曲外，也會對氧硒化鋅的生命期造成很大的影響。這個複雜的生命期衰減曲線可用柯爾洛希 (Kohlrausch) 的延伸性指數定律來描述，並可用電子的跳躍遷移模型做很好的解釋。除此之外，我們還發現隨著溫度升高，延伸參數 (β) 會出現先下降後上升的情形。這個結果反應了載子會因溫度上升而改變載子復合的機制。

Time-resolved photoluminescence of isoelectronic $ZnSe_{1-x}O_x$ semiconductors

Student : Hui-Lin Chung **Advisor : Prof. Wu-Ching Chou**

Institute of Electrophysics

National Chiao Tung University

Abstract

Oxygen in $ZnSe_{1-x}O_x$ acts as an isoelectronic trap that captures excitons and complicates the carrier relaxation paths. This study explores the influence of O on the carrier dynamics in $ZnSe_{1-x}O_x$ (O content up to 5.3 %) by using temperature-dependent photoluminescence (PL) and time-resolved PL spectroscopy. Incorporating oxygen not only causes large band-gap bowing but also strongly affects the emission lifetime of $ZnSe_{1-x}O_x$. Kohlrausch's stretched exponential law and hopping-transport model correlate well with the complex decay traces. Moreover, as the temperature increases, the stretching exponent β initially decreases and then monotonically increases. The results reflect a thermally activated transfer mechanism of carrier recombination.

Acknowledgement

兩年的研究所生活在不知不覺中就要走到了尾聲，這兩年在交大的日子，讓我認識了很多新朋友，也從研究室中學到了很多寶貴的經驗和知識，讓我獲益良多。

這兩年研究所的生涯，首先我要由衷的感謝我的指導老師周武清教授，提供了我在實驗上的很多資源，並且耐心的教導我，給予了我很多有用的建議。尤其在待人處事上，周老師也給了我很多良好的示範，我想這些都會讓我在未來受用無窮。另外，非常感謝徐子民老師、綦振瀛老師、陳衛國老師以及張文豪老師在研究上給予我寶貴的意見。其中，特別感謝綦振瀛老師提供了這套實驗的樣品，讓這份研究得以完成。同時，我也要特別感謝這兩年來帶領我的彥丞學長，因為學長對研究的精神與經驗，我的研究才能順利的完成，尤其在每次的討論過程中都讓我學習到很多，真的很感謝學長這兩年來耐心的教導與帶領。

接下來還要感謝實驗室的學長姐們，感謝文忠學長、瑞泰學長、崑峯學長、李寧學長瑞雯學姊和威智學長，感謝你們能夠分享許多自己的研究經驗以及給我的指導與鼓勵。感謝偉仕學弟和大陸同胞高昆，因為有你們的陪伴和幫忙，讓我的實驗室生活變得更多采多姿。感謝崑峯學長帶著我一起去當普物實驗助教，因為你我才能很快的適應實驗室和交大的生活，在這邊預祝學長資格考順利過關。還有要感謝現在正在台積電的瑞雯學姊，在實驗室裡陪我談天說地，並且會在節日時給我有趣的小禮物及點心，讓我既驚喜又感動，祝福學姐在台積電能順順利利賺大錢。

最後，我要感謝我的家人，爸爸、媽媽、妹妹，感謝你們的支持和陪伴，謝謝你們總是為我著想，並用寬容的心體貼我、包容我，讓我能在交大順利的完成學業。我還要謝謝我的好朋友們，種子、資雲、柚子以及雷丘，謝謝你們在我忙碌的生活中為我打氣，也謝謝你們願意聽我抱怨，陪我玩樂。並且特別感謝柚子和雷丘，因為有你們的幫忙，我才能不用到處來回奔波，專心的完成這份論文，所以在此也將這份完成論文的喜悅與你們分享。

Contents

List of Figures

List of Tables

Chapter 1 Introduction

In recent years, highly mismatched alloys (HMAs) have been studied extensively both experimentally and theoretically due to their unique and interesting optical properties [1-10]. HMAs are a class of material in which the constituent anion element is partially replaced by an isovalent element with very dissimilar properties, such as size and electronegativity. The most extensively studies HMAs to date are III-V-N systems, such as N in GaAs and GaP, where N plays an isoelectronic impurity. In the case of GaAsN, for example, the electronegativity (size) of N is much larger (smaller) than that of As. The highly mismatched electronegativity and size lead to a profound effect on optical and electronic properties. These properties include, for example, giant and asymmetric band-gap bowing, significant increase of the electron effective mass, the appearance of a new optical transition (E_+), nonlinear pressure dependence of the band gap, and a reduced temperature dependence of the band gap [1-10].

In II-VI Oxygen alloys, incorporating Oxygen into ZnSe reveals a similar highly mismatched effect in $ZnSe_{1-x}O_x$ [11]. Comparing O and Se, the electronegativity (size) of O is much larger (smaller) than that of Se. The electronegativity (size) is 3.5 (0.66 Å) and 2.4 (1.17 Å) for O and Se element, respectively. Therefore, the dramatic changes of the optical properties in $ZnSe_{1-x}O_x$ can be expected. These changes in electronic band structure deviate

greatly from the predictions of the virtual crystal approximation (VCA). Previously, the large band-gap bowing behavior of $ZnSe_{1-x}O_x$ was described using a bowing parameter. Nabetani *et al.* found that the band-gap bowing parameter of $ZnSe_{1-x}O_x$ is about 8 eV in the Se-rich region [12]. However, Iwata *et al.* found that the bowing parameter is about 12 eV in O-rich region [13]. These results imply an asymmetric band-gap bowing, reflecting that single bowing parameter cannot describe the band-gap bowing of $ZnSe_{1-x}O_x$ throughout the entire O concentration.

Recently, the band anticrossing (BAC) model was proposed to explain the change of electronic band structure of HMAs [5]. In the case of II-VI-O system, the BAC model can be considered as an interaction of two energy states: defect state of O and the extended conduction band state of the host matrix. The interaction of the two types of states can be treated as a perturbation which leads to the following eigenvalue problem:

$$\begin{vmatrix} E - E_M & V_{OM} \\ V_{OM} & E - E_O \end{vmatrix} = 0,$$

where E_M is the band gap of the host matrix, E_O is the O defect state relative to the valence band, and V_{OM} is the parameter describing the strength of the interaction between them. By solving the eigenvalue problem, the two solutions can be written as,

$$E_{\pm} = \frac{1}{2}\left(E_O + E_M \pm [(E_O - E_M)^2 + 4V_{OM}^2]^{\frac{1}{2}}\right).$$

It has been shown previously that the square of the matrix is proportional to the concentration of Oxygen atoms. Consequently, the strength of the coupling V_{OM} can be described as

$$V_{OM} = C_{OM} x^{1/2},$$

where C_{OM} is a constant dependent on the semiconductor matrix, and x is the concentration of Oxygen [14-15]. Shan *et al.* found that the BAC model explains well in the composition and pressure dependence of the band gap in $ZnSe_{1-x}O_x$ with C_{OM} = 1.8 ± 0.3 eV [16]. However, Polimeni *et al.* found no effect of oxygen on the temperature dependence of band gap in $ZnSe_{1-x}O_x$ (x = 0.23 - 0.90 %), which deviates from the prediction of the BAC model [17]. Accordingly, we will investigate the temperature dependence of photoluminescence (PL) on isoelectronic $ZnSe_{1-x}O_x$ semiconductors and compare the results with previous works.

Although much research efforts have been focused on isoelectronic $ZnSe_{1-x}O_x$ semiconductors, the influence of O on the decay dynamics in this material remains unexplored. Recently, we have studied the decay dynamics of isoelectronic $ZnSe_{1-x}Te_x$ semiconductors [18]. We demonstrated that the PL decay traces are correlated well with the Kohlrausch's stretched exponential law [19],

$$I(t) = I_0 \cdot e^{-(t/\tau)^{\beta}},$$

where τ is the PL lifetime and β is the stretching exponent varied from 0 to 1. The Kohlrausch law has been extensively used to describe numerous complex relaxation processes [20-26]. The stretched exponential decay behavior has also been observed in single colloidal semiconductor nanocrystals because of the presence of multinonradiative decay channels that surround the single nanocrystal [27]. In the study of $ZnSe_{1-x}Te_x$, the stretched exponential

decay is attributed to the presence of Te localized states, which provide multidecay paths in $ZnSe_{1-x}Te_x$. These results can be understood using energy transfer and the geometric random site hopping-transport model [18]. According to this model, the transport sites (N_0) and the trapping sites (N_T) distribute randomly in 3D space of a system, in which an electron can move among the transport sites in many different ways and be captured by a trap state. Based on the numerical simulations, Sturman *et al.* obtained that the value of the stretching exponent β decreases with the decreasing of N_0/N_T [28]. Accordingly, the applicability of the Kohlrausch law and exploring the effect of O on the carrier dynamics in $ZnSe_{1-x}O_x$ is important and of great interest. In this thesis, we study the carrier dynamics of isoelectronic $ZnSe_{1-x}O_x$ semiconductors with O composition up to 5.3 % by using PL and time-resolved PL (TRPL) spectroscopy.

This thesis is organized as follows. This chapter introduces the unusual physical properties of isoelectronic semiconductors. Chapter 2 introduces the PL and TRPL systems used in this thesis. Chapter 3 discusses the influence of O on the decay dynamics in $ZnSe_{1-x}O_x$ as functions of O concentration and temperature. Finally, Chapter 4 summarizes this thesis.

Chapter 2 Experimental Setup

In this chapter, the experimental systems used in this thesis are described. The experimental systems include photoluminescence (PL) system and time-resolved photoluminescence (TRPL) system.

2.1 Photoluminescence (PL) System

The experimental setup of the PL system is shown in Figure 2.1. The samples were loaded on the cold finger of a closed cycle cryostat and the temperature was controlled between 10 and 300 K. The GaN pulsed laser (405 nm) was used as an excitation source with the excitation power of about 1 mW. The incident laser beam was focused on the sample by a convex lens (L_1). The PL signal from the sample was collected by a set of convex lenses (L_2 and L_3) and guided to spectrometer. The signal was dispersed by a SPEX 1404 0.85 m double-grating spectrometer and detected using photomultiplier tube (PMT). The spectrometer was controlled by a computer, which was used to store and plot the collected data. An He-Cd (325 nm) laser was used to carry out the excitation power-dependent PL measurements, and a density filter was added in front of the laser to adjust the laser power.

2.2 Time-Resolved Photoluminescence (TRPL) System

TRPL system was used to study the decay dynamics of excitons. The experimental setup of TRPL system is similar to the PL system and shown in Figure 2.2. The GaN pulsed laser (405 nm) with a pulse width of 200 ps and repetition rate of 10 MHz was used as an excitation source. The laser beam was focused on the sample by a convex lens (L_1). The combination lenses (L_2 and L_3) guide the PL signal to the iHR550 spectrometer, which was equipped with a high speed PMT to detect the signal. The signal was further analyzed by a computer with a time-correlated single photon counting method. The overall temporal resolution of the TRPL measurement is about 200 ps.

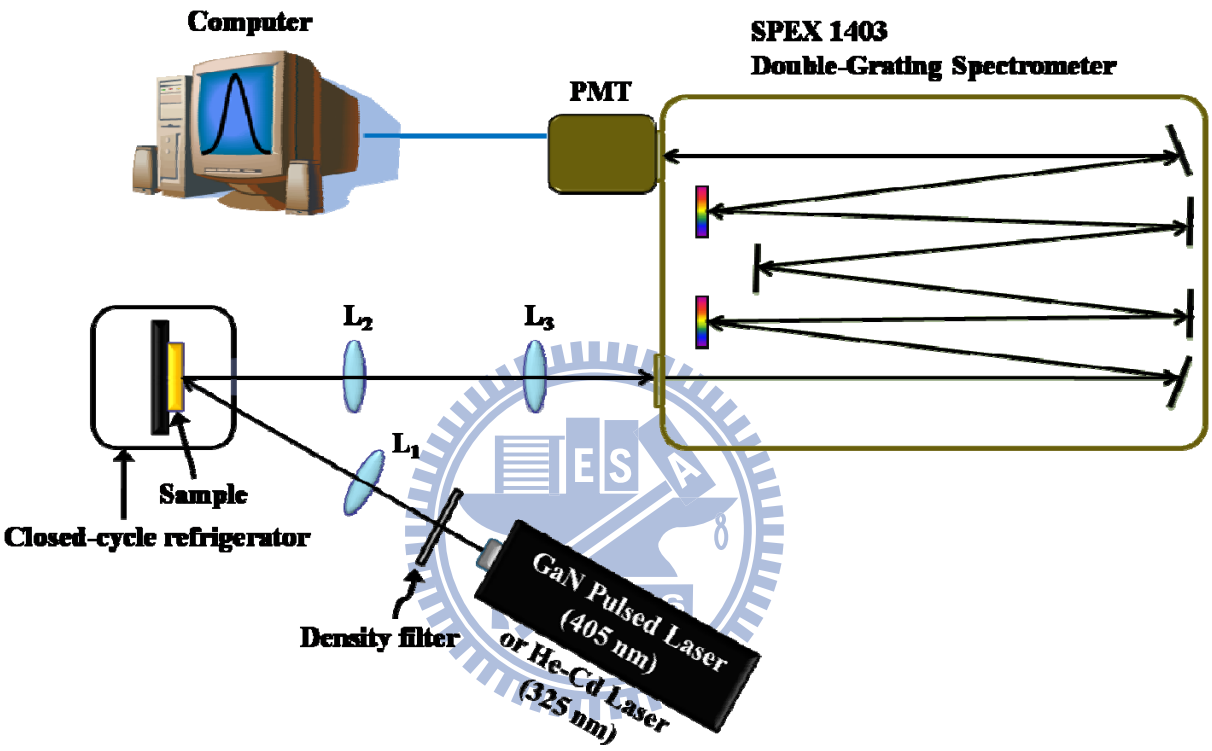

Fig. 2.1. Experimental setup of PL system.

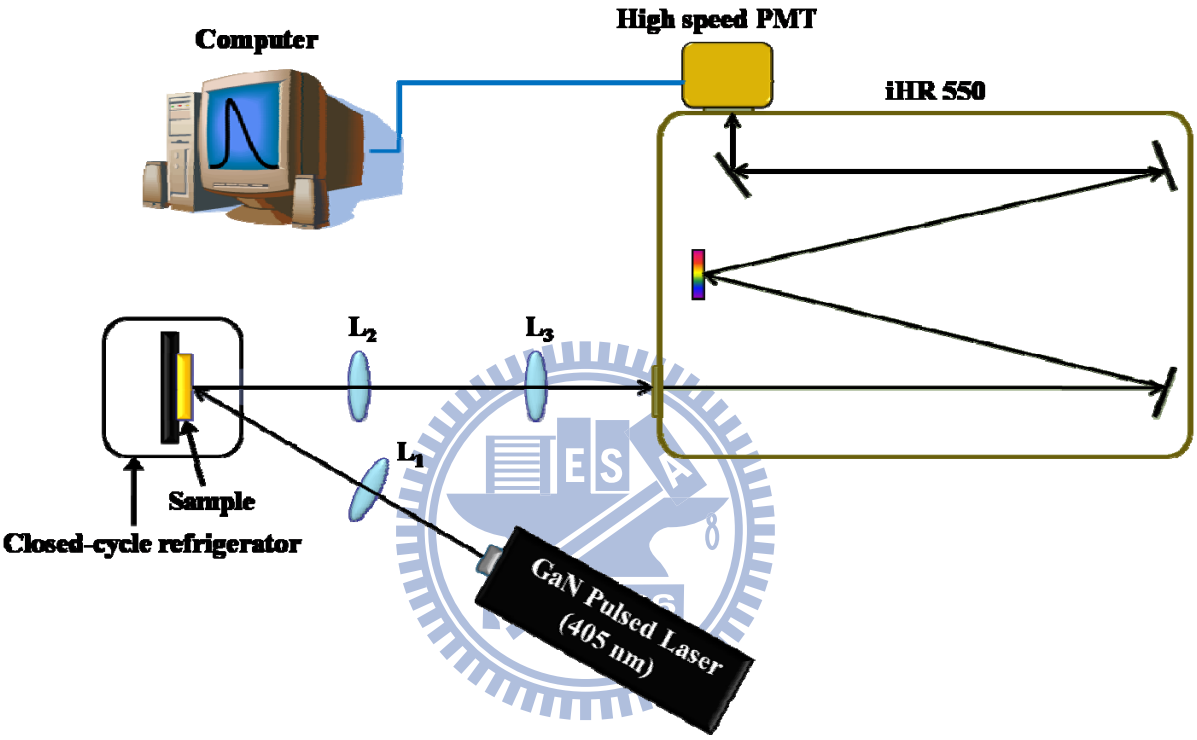

Fig. 2.2. Experimental setup of TRPL system.

Chapter 3 Results and Discussion

In this chapter, we study the carrier dynamics of $ZnSe_{1-x}O_x$ with O composition up to 5.3% using PL and TRPL measurements. In section 3.1, we will discuss the results of temperature-dependent PL measurements. In section 3.2, the dependence of both temperature and monitored energy on the decay dynamics of $ZnSe_{1-x}O_x$ will be investigated.

3.1 Photoluminescence Study of $ZnSe_{1-x}O_x$

$ZnSe_{1-x}O_x$ (x = 0, 0.027, and 0.053) films were grown by RF-plasma assisted molecular beam epitaxy on (001) GaAs substrates after the deposition of a 100 nm-thick ZnSe buffer layer. The thicknesses of all films were fixed at around 0.5 μm and the O concentration was determined by x-ray diffraction. [29]. Figure 3.1 shows the normalized PL and transmission (T) spectra of $ZnSe_{1-x}O_x$ (x = 0, 0.027, and 0.053) at 10 K. Clearly, a sharp near-band-edge emission of ZnSe peaked at about 2.80 eV is observed. When O is substituted into ZnSe, the PL emissions shift toward lower energies, 2.52 and 2.42 eV for x = 0.027 and 0.053, respectively. As the O concentration is increased, the emissions become broader and asymmetric. This result can be attributed to the alloy fluctuations or O clustering. Figure 3.2(a) presents the excitation power-dependent PL spectra for $ZnSe_{0.973}O_{0.027}$. Increasing the laser power by four orders of magnitude, a significant blueshift (~ 8 meV) in PL peak energy is investigated, which implies carrier localization and filling effect. A blueshift by about 8 meV

is also found in $ZnSe_{0.947}O_{0.053}$ in the same excitation power range, indicating that the broad emissions of $ZnSe_{1-x}O_x$ are attributable to localized excitons (LE).

To clarify further the dependence of temperature on the carrier dynamics in $ZnSe_{1-x}O_x$, temperature-dependent PL measurements are performed. Figure 3.3 and Figure 3.4 show the temperature-dependent PL spectra of $ZnSe_{1-x}O_x$ for x = 0.027 and 0.053, respectively. The PL peaks exhibit an S-shaped energy shift with increasing temperature, which is a typical feature of carrier localization effect. At 10 K, a LE emissiom which is determined from the power-dependent PL measurements can be observed. With increasing temperature, the emission from LE shifts toward lower energy and becomes broader. When the temperature is increased further, the LE peak quickly thermally quenches and another peak appears at high energy shoulder between 80 and 100 K. As the temperature is increased above 100 K, the high-energy peak becomes dominant and shift to lower energy. This emission shows a normal Gaussian shape, while that from LE exhibits an asymmetric shape with a low-energy tail and a sharp high-energy cutoff. Moreover, the emission yields no obvious energy shift over a range of excitation power by three orders of magnitude as shown in Figure 3.2(b). Based on these observations, the emission at the high energy shoulder is attributed to free excitons (FE) thermally detrapping from the isoelectronic O trap states.

Figure 3.5(a) and 3.5(b) depict the corresponding temperature-dependent PL peak energies for x = 0.027 and 0.053, respectively. As shown in the figures, the FE peak energies

agree well with the empirical Varshni fitting (solid curve),

$$E_g(T) = E_g(0) - \alpha T^2 / (\beta + T), \tag{1}$$

where $E_g(0)$ is the band gap at 0 K, and α and β are the Varshni fitting parameters, listed in Table 3.1. Increasing the O concentration, α decreases from 1.20 to 0.72 meV/K for $x = 0$ and 0.053, respectively. The experimental result indicates a decreased dependence of the $ZnSe_{1-x}O_x$ band gap on temperature. The temperature-dependent band gap energy of $ZnSe_{1-x}O_x$ can also be fitted using the BAC model [5],

$$E_g(T) = \frac{1}{2}\left[E_O + E_M(T) - \left\{\left[E_O - E_M(T)\right]^2 + 4C_{OM}^2 x\right\}^{1/2}\right], \tag{2}$$

where E_O and $E_M(T)$ are the energies of the O level and the ZnSe conduction band (CB) edge relative to the top of the valence band (VB), respectively. $E_M(T)$ can be obtained by Eq. (1) for ZnSe. C_{OM} is a parameter describing the strength of the interaction between the O level and the ZnSe CB states. The result of theoretical calculation is represented in Figure 3.5 by dashed curve. The fitting parameters are listed in Table 3.1. As shown in Figure 3.5(a) and 3.5(b), the FE energies are in good agreement with BAC model. The fitted band gap energy using Varshni equation and BAC model at 10 K approaches the value measured from transmission measurement (Figure 3.1). The above observations provide additional evidences to the FE emissions. Figure 3.6 plots the band gap energy of $ZnSe_{1-x}O_x$ as a function of O concentration at 300 K. Experimental results from previous studies are also included [16]. The band gap energy decreases with increasing x. The bang gap behavior can be fitted by BAC

model with E_O = 2.90 eV and C_{OM} = 1.82 eV. The values are within the error of previous study, which found E_O = 2.9 ± 0.02 eV and C_{OM} = 1.8 ± 0.3eV [16].

Based on the above observations, we can conclude that the unique optical properties of $ZnSe_{1-x}O_x$ can be well explained using BAC model. This result is different from the previous study of Polimeni *et al.*, who found that the temperature dependence of the band gap in $ZnSe_{1-x}O_x$ is independent from O concentration[17]. The reason why their experimental results are inconsistent with the prediction of the BAC model might be the poor sample quality or the relative low O concentration (O content less than 1.0 %).

3.2 Time-resolved Photoluminescence Study of $ZnSe_{1-x}O_x$

In order to explore the effect of O on the decay dynamics in $ZnSe_{1-x}O_x$, the TRPL measurements are performed. Figure 3.7 displays the TRPL spectra of $ZnSe_{1-x}O_x$ (x = 0.027 and 0.053) monitored at the PL peaks and 10 K. Obviously, several interesting findings can be drawn. (i) The PL decay profiles exhibit non-single-exponential decay and can be decomposed into a fast (initial) and a slow (tail) component. Moreover, the fast component is mono-exponential decay, while the slow component is stretched-exponential behavior. (ii) The PL decay rate is an order of magnitude slower than that of ZnSe (~ 5.0 ns^{-1}). (iii) The PL lifetime of slow component significantly increases with the O concentration. These unique optical properties are signatures of ZnSe-based isoelectronic semiconductors [18], implying complicated carrier dynamics. Quantitatively, the decay curves are fitted by using the following equation,

$$I(t) = A_1 \cdot e^{-t/\tau_1} + A_2 \cdot e^{-(t/\tau_2)^{\beta}} , \qquad (3)$$

where τ_1 and τ_2 is the exciton lifetime of fast and slow component respectively, and β is the stretching exponent ranging from 0 to 1. This stretching exponent is a measure of the relaxation rates involved in the PL decay process where a smaller β means a broader rate distribution. The fitted τ_1 is about 850 ps for both samples; τ_2 (β) is about 2.8 ns (0.96) and 4.1 ns (0.93) for x = 0.027 and 0.053, respectively. Increasing the O concentration increases τ_2 and decreases β, implying that the slow decay originates from O-related LE. This is because an

increasing number of isoelectronic O traps provides multidecay paths for the excitons [18]. The suggestion is consistent with the hopping-transport model, in which the concentrations of transport and trapping sites determine the stretching exponent [28].

To verify the suggestions, Figure 3.8(a) and 3.8(b) show the TRPL spectra at 10 K and various monitored energies for x = 0.027 and 0.053, respectively. Decreasing the monitored energy, the decay time from the slow component significantly increases, while the decay time from the fast component is insensitive to energy. For x = 0.027, τ_2 (β) is around 2.4 ns (0.97) and 4.7 ns (0.76) at 2.55 and 2.43 eV, respectively. For x = 0.053, τ_2 (β) is around 2.8 ns (0.97) and 7.4 ns (0.70) at 2.44 and 2.32 eV, respectively. In accordance with the asymmetric linewidth broadening, the above results can be ascribed to exciton energy transfer among isoelectronic O traps. The TRPL image in Fig 3.9 reveals the dynamics of energy transfer in $ZnSe_{0.973}O_{0.027}$. Within the initial few nanoseconds after excitation, the emission is peaked at 2.52 eV. As time passes, an energy redshift is clearly observed, revealing that some of the LE transfer to deeper traps. Moreover, the decay profile at high energy exhibits mono-exponential decay, whereas that at low energy is a stretched-exponential function, implying that the effect of LE can be neglected at high energy region. This phenomenon becomes even more pronounced upon recording of the higher energy emissions. Therefore, the fast decay discussed herein can be ascribed to free excitons (FE).

For comparing S-shaped feature with the decay traces, Figure 3.10 and Figure 3.11

display the temperature-dependent TRPL spectra of $ZnSe_{1-x}O_x$ (x = 0.027 and 0.053). According to these figures, increasing the temperature significantly quenches the lifetime of slow component. As the temperature is increased above 100 K, the slow decay component is eliminated and the fast decay dominates the entire decay profile. Moreover, the bending of the logarithmic decay curve, *i.e.* a reduction in β, initially becomes more pronounced with increasing temperature up to 70 K and then gradually diminishes, *i.e.* the β starts to increase. To get a more quantitative measure of the β, the decay curves are fitted with Eg. (3). The stretching exponent β as a function of temperature is displayed in the inset in Figure 3.10 and Figure 3.11 for x = 0.027 and 0.053. Increasing the temperature initially decreases β to a minimum at 70 K and then monotonically increases. This phenomenon can be explained by the corresponding configuration coordinate diagram schematically shown in Figure 3.12(a). At the lowest temperature (10 K), electrons that are generated initially in the free state hop among proximal transport and trapping sites and recombine with the isoelectronic O traps (channel 1). With increasing temperature these less mobile electrons are imparted with additional energy that allow hopping to deeper trap states (channel 2), causing a rapid redshift in the LE peak and a reduction of β. Simultaneously, as the temperature approaches 70 K, portions of trapped electrons are thermally activated back to populate the higher energy states (channel 3), leading to a significant PL linewidth broadening at the high energy shoulder. At still higher temperatures, an increasing number of electrons gain sufficient energy to

delocalize into the free state (channel 4) and recombine, explaining the increase in β and the blueshift of the PL peaks. Above 100 K, the slow decay component disappears because FE dominates the recombination, resulting in a monotonic PL energy redshift with the temperature. The delocalization effect is further verified by the TRPL image of $ZnSe_{0.947}O_{0.053}$ at 80 K. In Figure 3.12(b), as time passes an energy redshift at low-energy peak is observed due to the recombination from traps. However, the high-energy peak exhibits no obvious energy shift with time, reflecting the recombination of thermally delocalized FE.

Table 3.1 Fitting parameters from the Varshni equation and the BAC model.

O concentration (x)	Varshni equation			BAC model	
	$E_g(0)$ (eV)	α (meV/K)	β (K)	E_O (eV)	C_{OM} (eV)
0	2.81	1.20	495	-	-
0.027	2.54	0.78	495	2.90	1.89
0.053	2.44	0.72	495	2.90	1.78

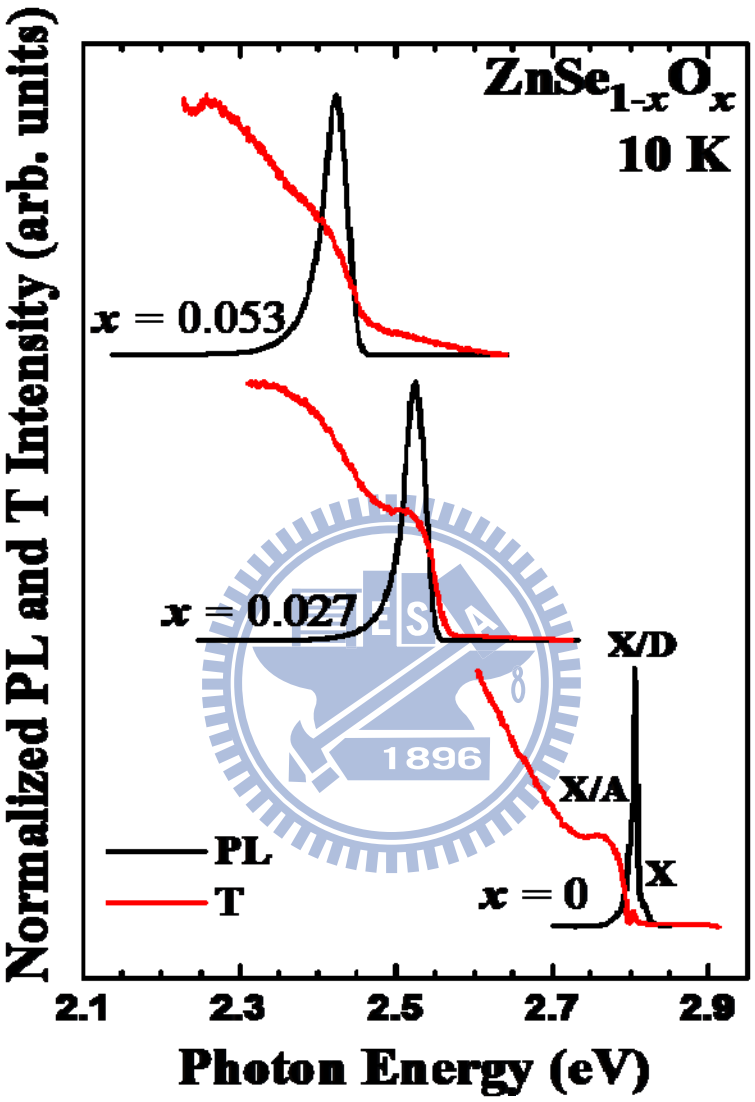

Fig. 3.1. Normalized PL and transmission spectra of $ZnSe_{1-x}O_x$ at 10 K.

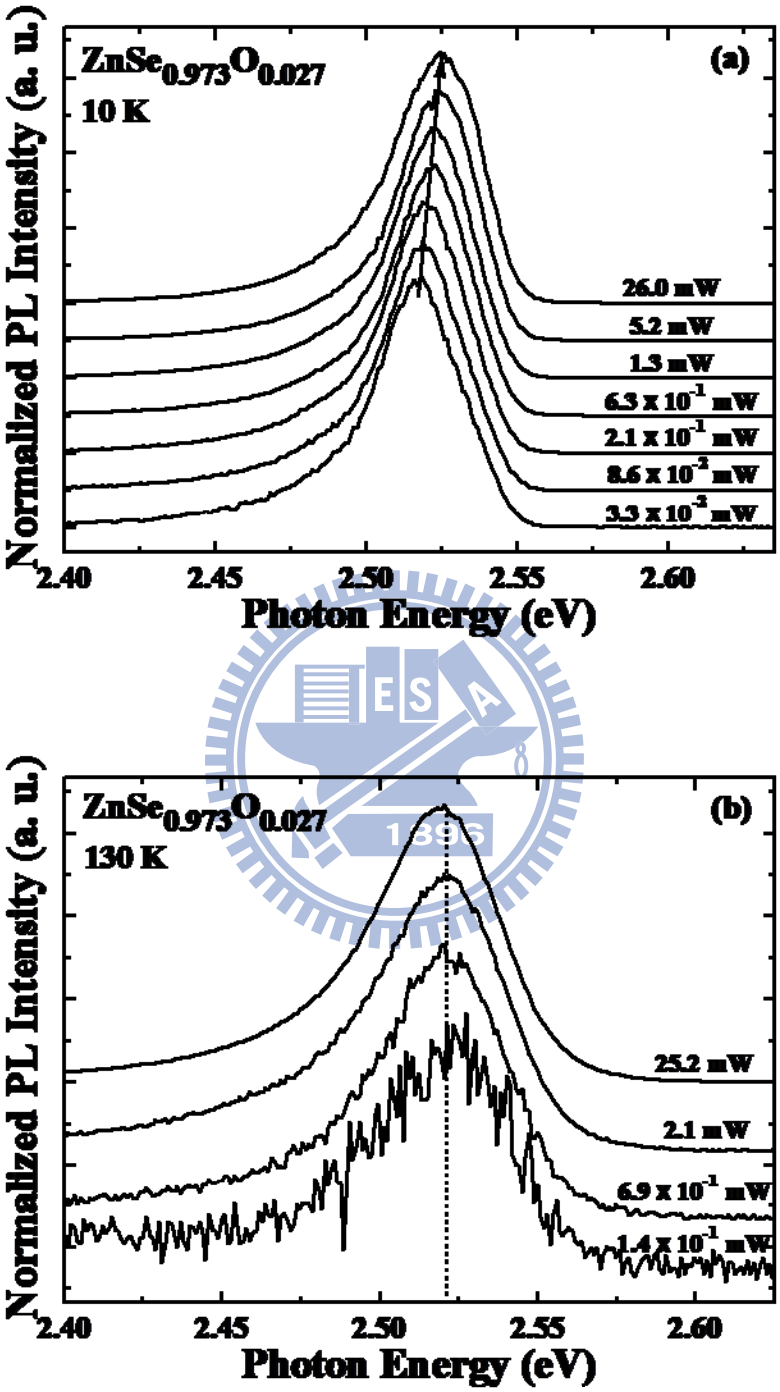

Fig. 3.2. Excitation power-dependent PL spectra for $ZnSe_{0.973}O_{0.027}$ at (a) 10 K and (b) 130 K.

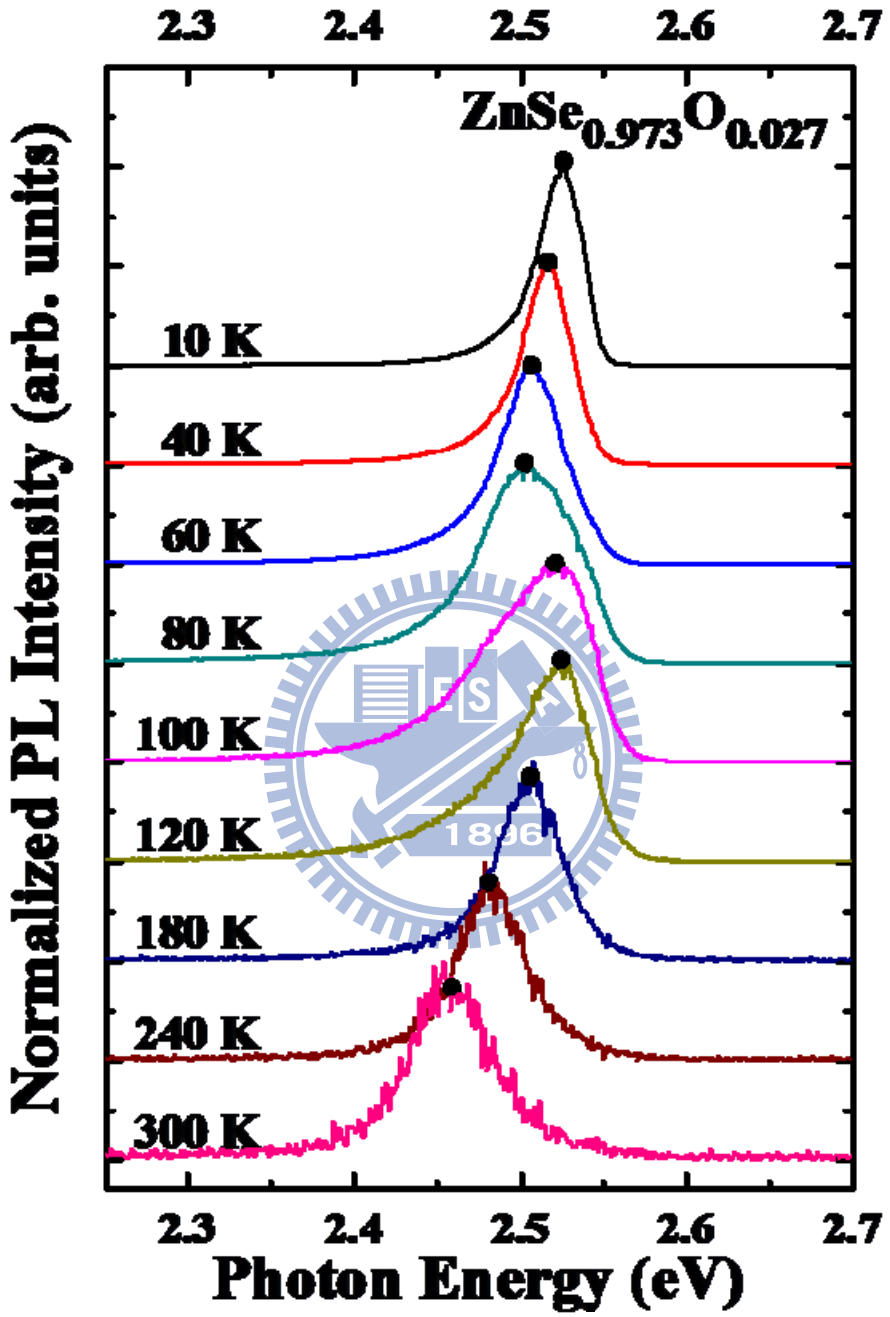

Fig. 3.3. Temperature-dependent PL spectra of $ZnSe_{0.973}O_{0.027}$.

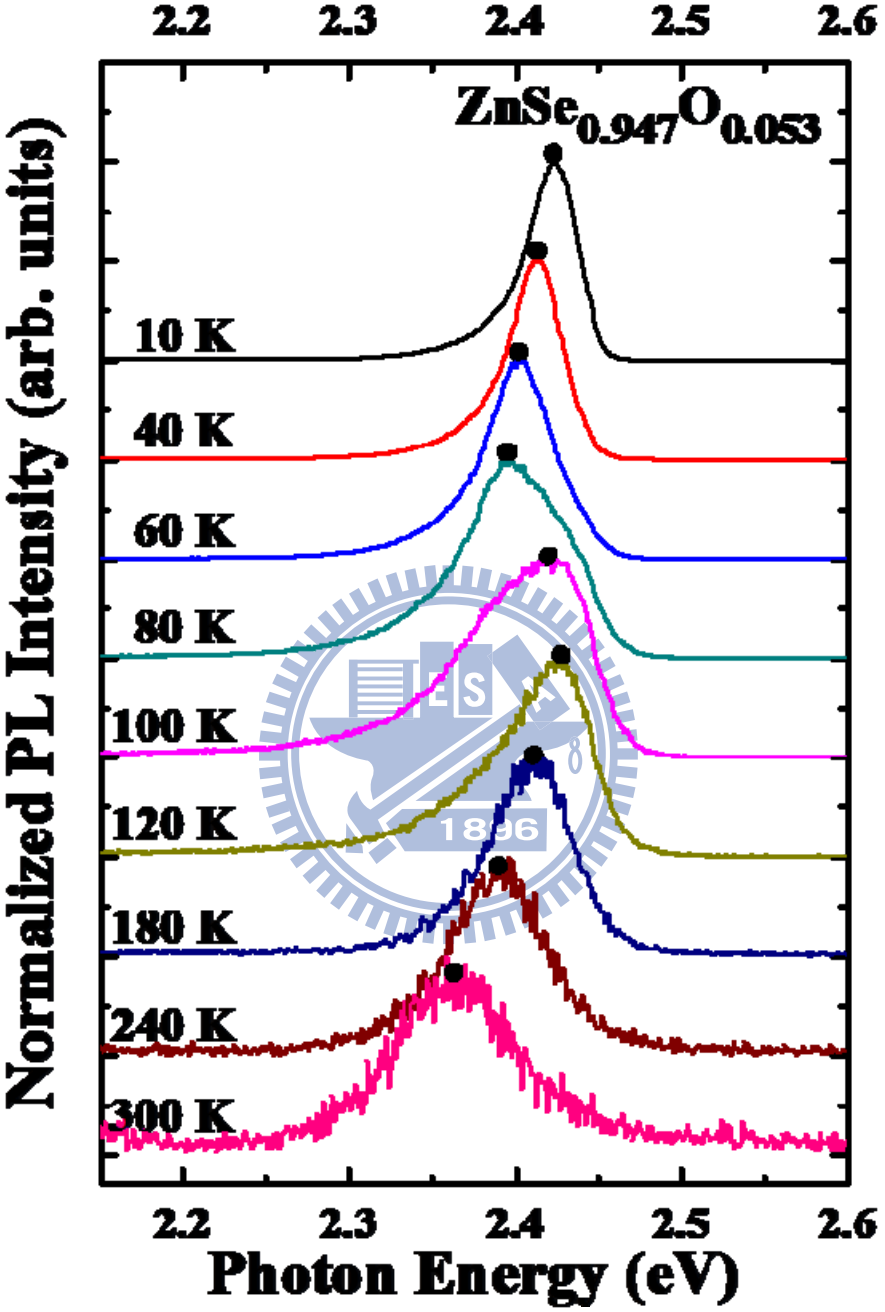

Fig. 3.4. Temperature-dependent PL spectra of $ZnSe_{0.947}O_{0.053}$.

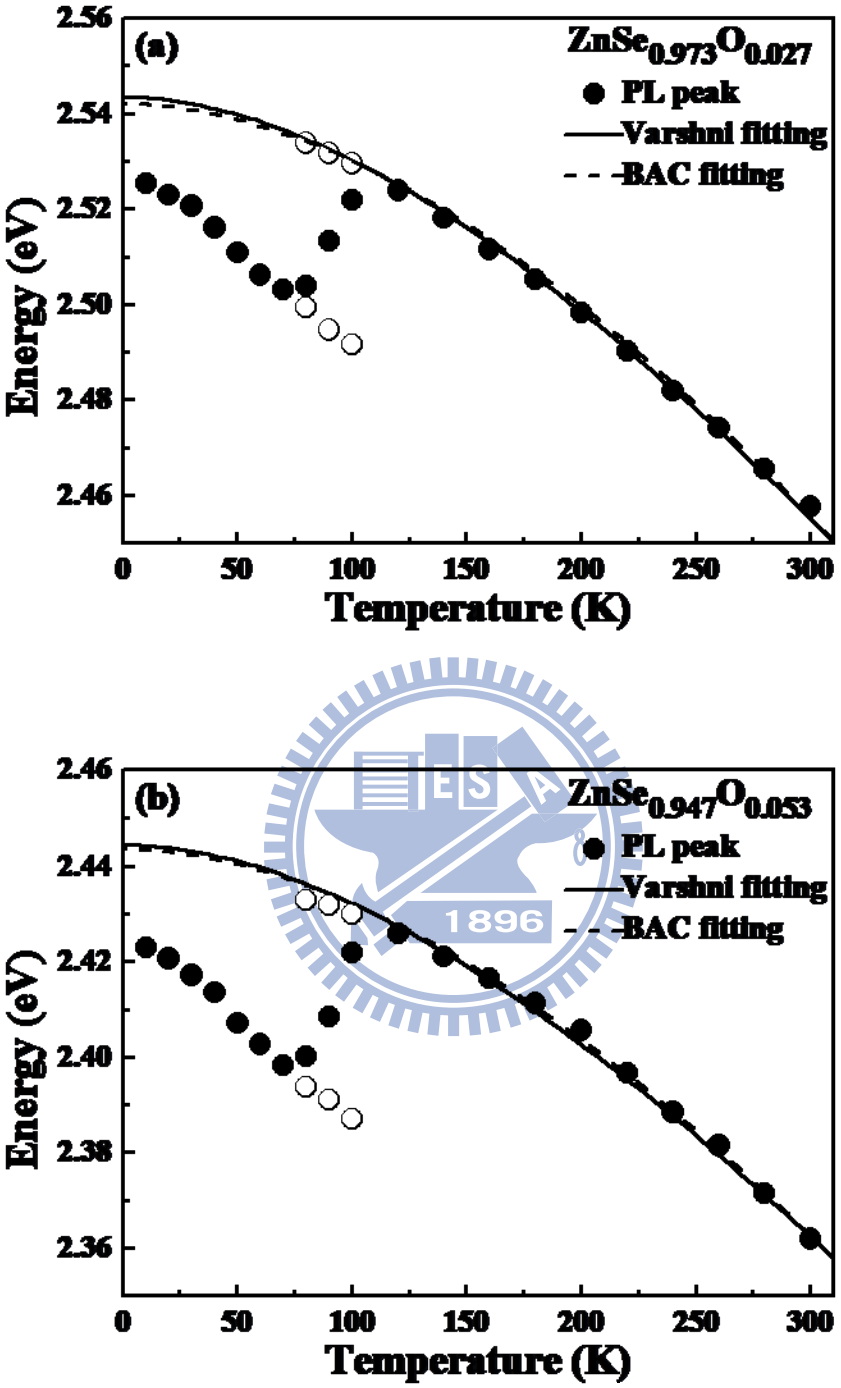

Fig. 3.5. Temperature-dependent PL peak energies for (a) $ZnSe_{0.973}O_{0.027}$ and (b) $ZnSe_{0.947}O_{0.053}$. The solid and dashed curves present the fits from the Varshni equation and the BAC model, respectively. The open circles denote the PL peak energy fitted by two Gaussian functions.

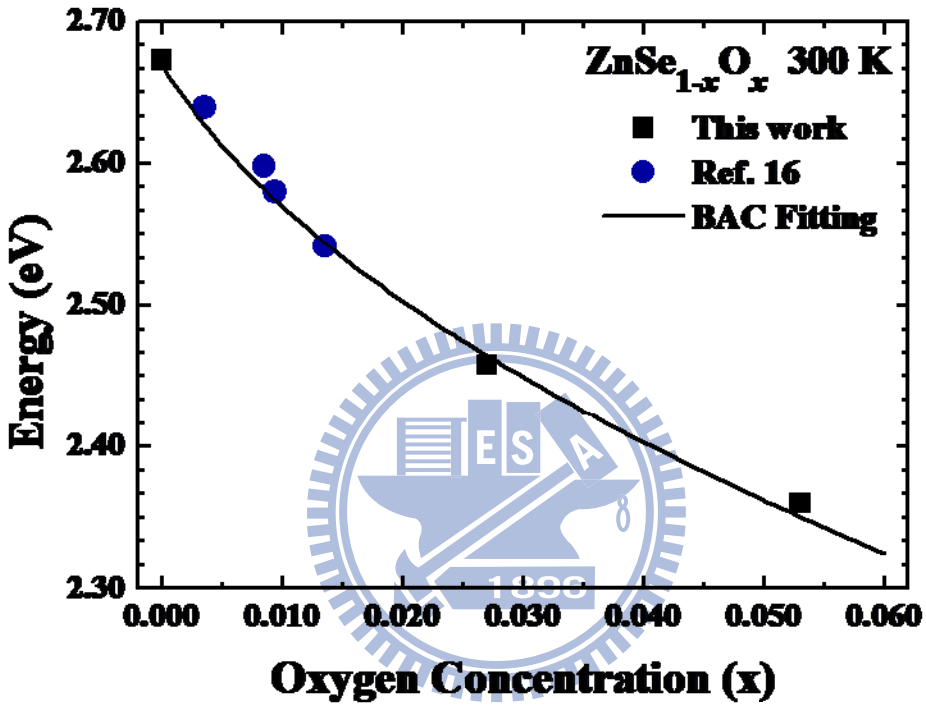

Fig. 3.6. Band gap energy of $ZnSe_{1-x}O_x$ as a function of O concentration at 300 K. The black squares mark the PL energy in this work, the blue circles mark the value from photoreflectance in Ref. 16, and the black curve shows the best fit by BAC model.

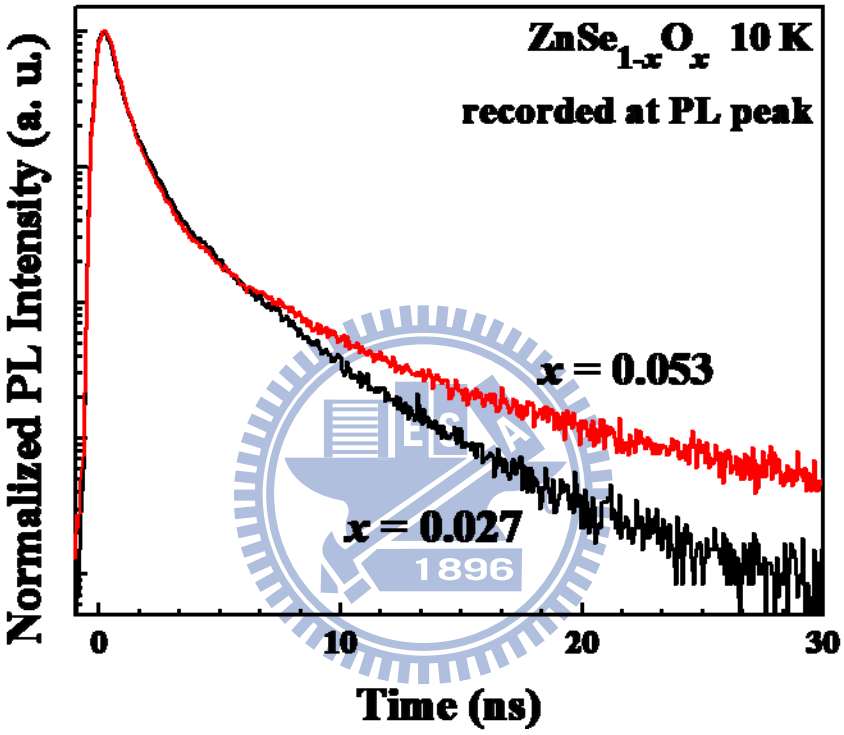

Fig. 3.7. TRPL spectra at 10 K of $ZnSe_{1-x}O_x$ (x = 0.027 and 0.053).

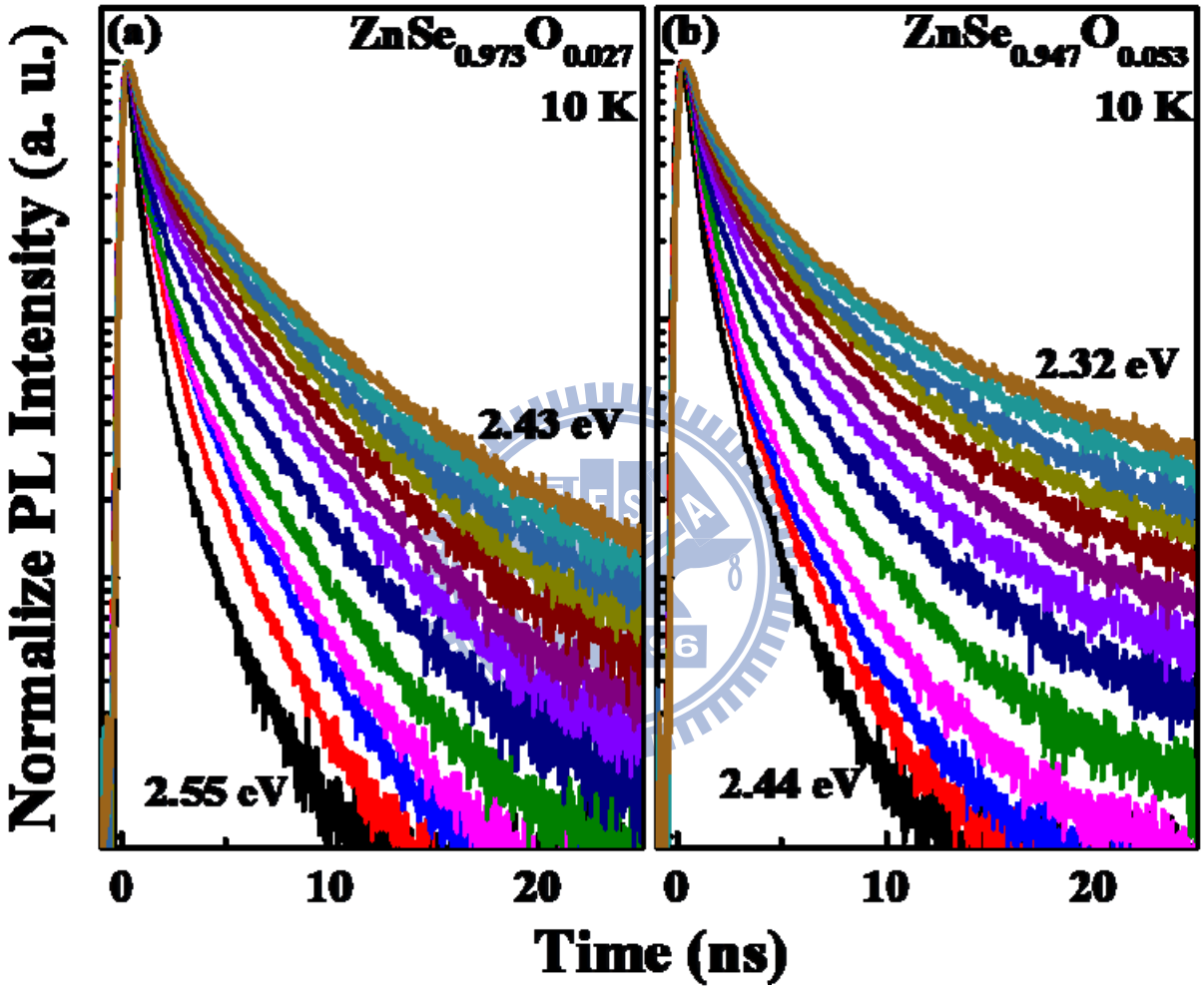

Fig. 3.8. TRPL spectra at 10 K as a function of monitored energies for (a) x = 0.027 and (b) 0.053.

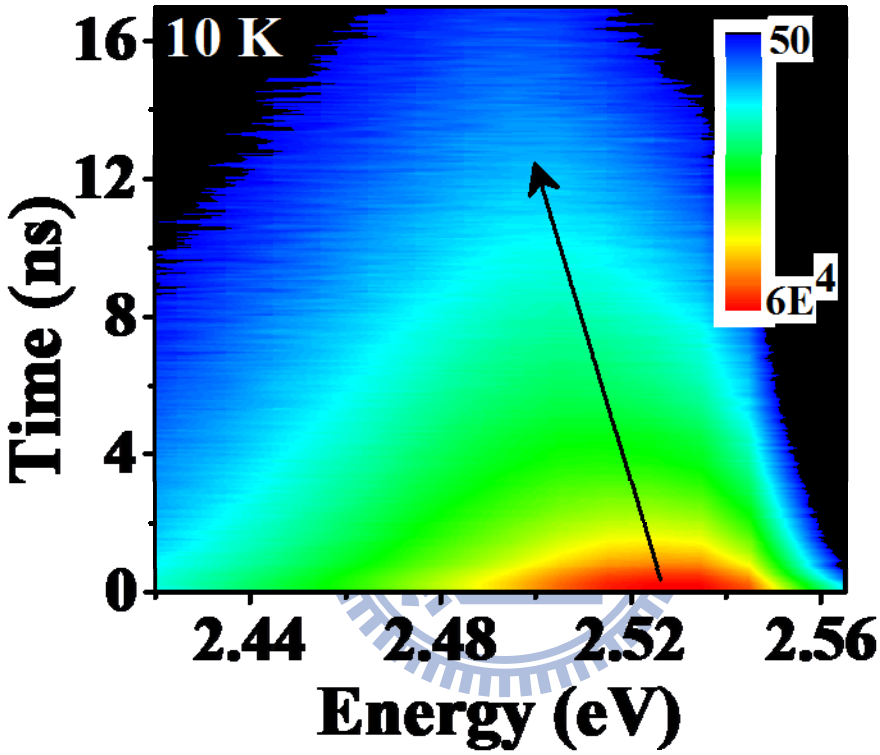

Fig. 3.9. TRPL image of $ZnSe_{0.973}O_{0.027}$ at 10 K.

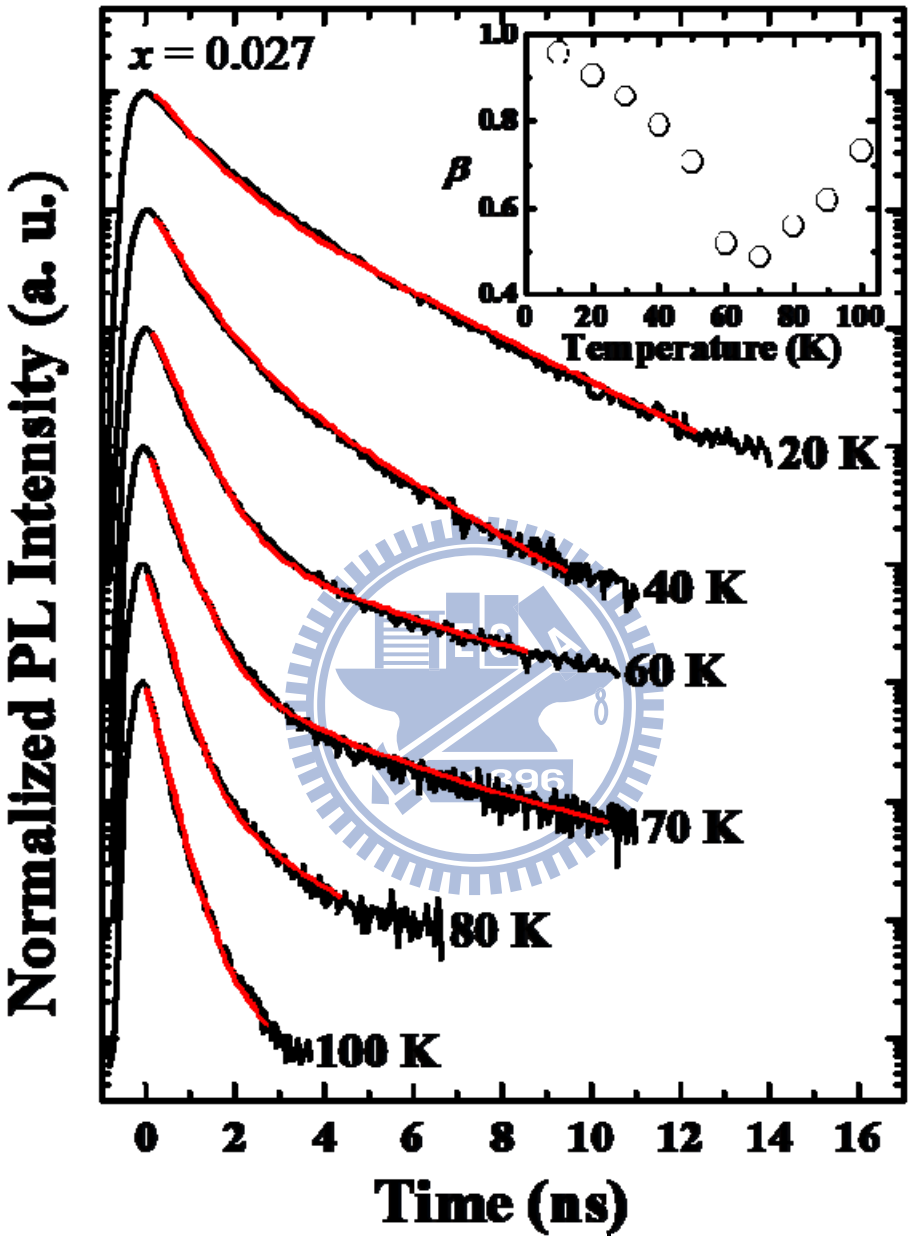

Fig. 3.10. Temperature-dependent TRPL spectra of $ZnSe_{0.973}O_{0.027}$ and the corresponding stretching exponent β (inset).

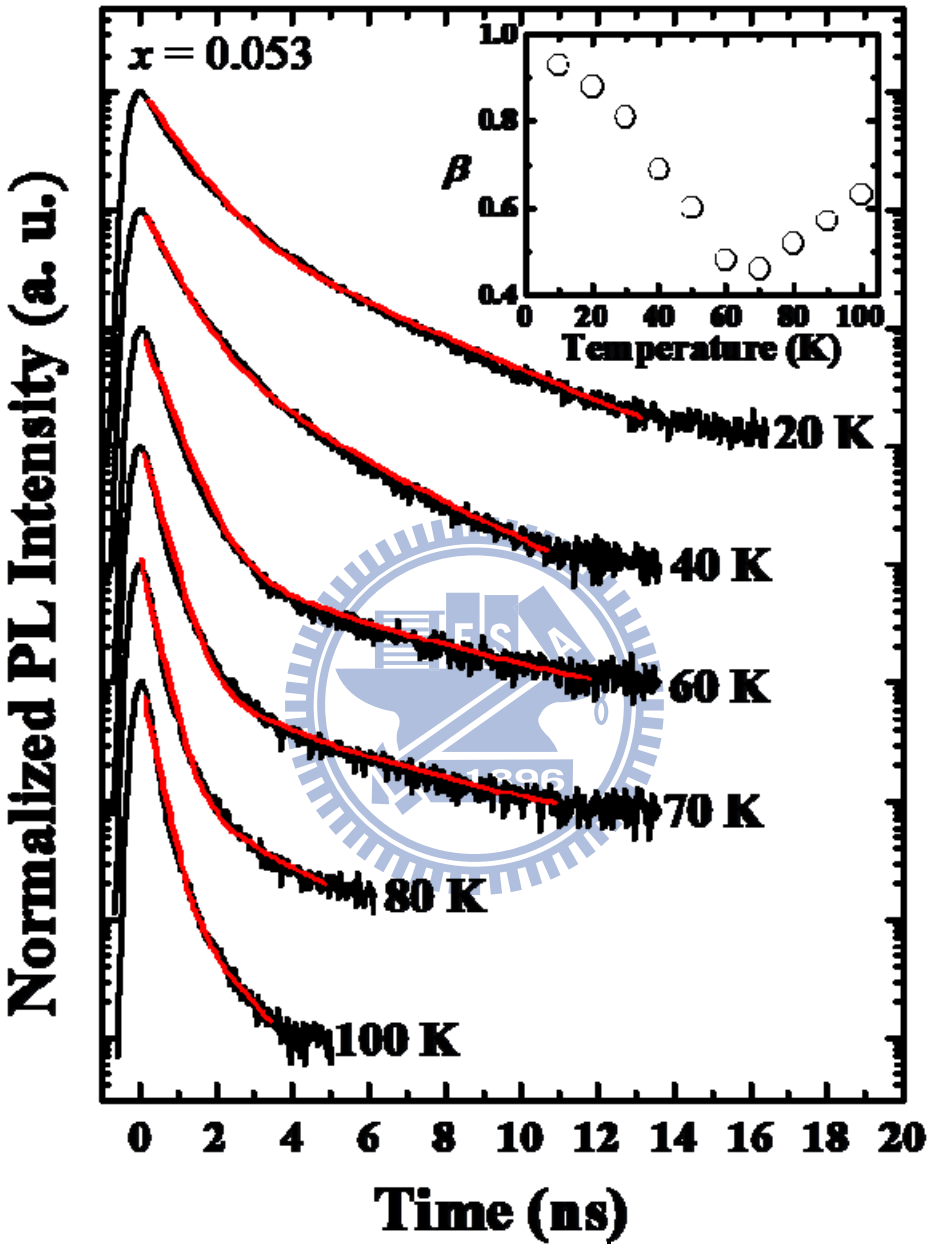

Fig. 3.11. Temperature-dependent TRPL spectra of $ZnSe_{0.947}O_{0.053}$ and the corresponding stretching exponent β (inset).

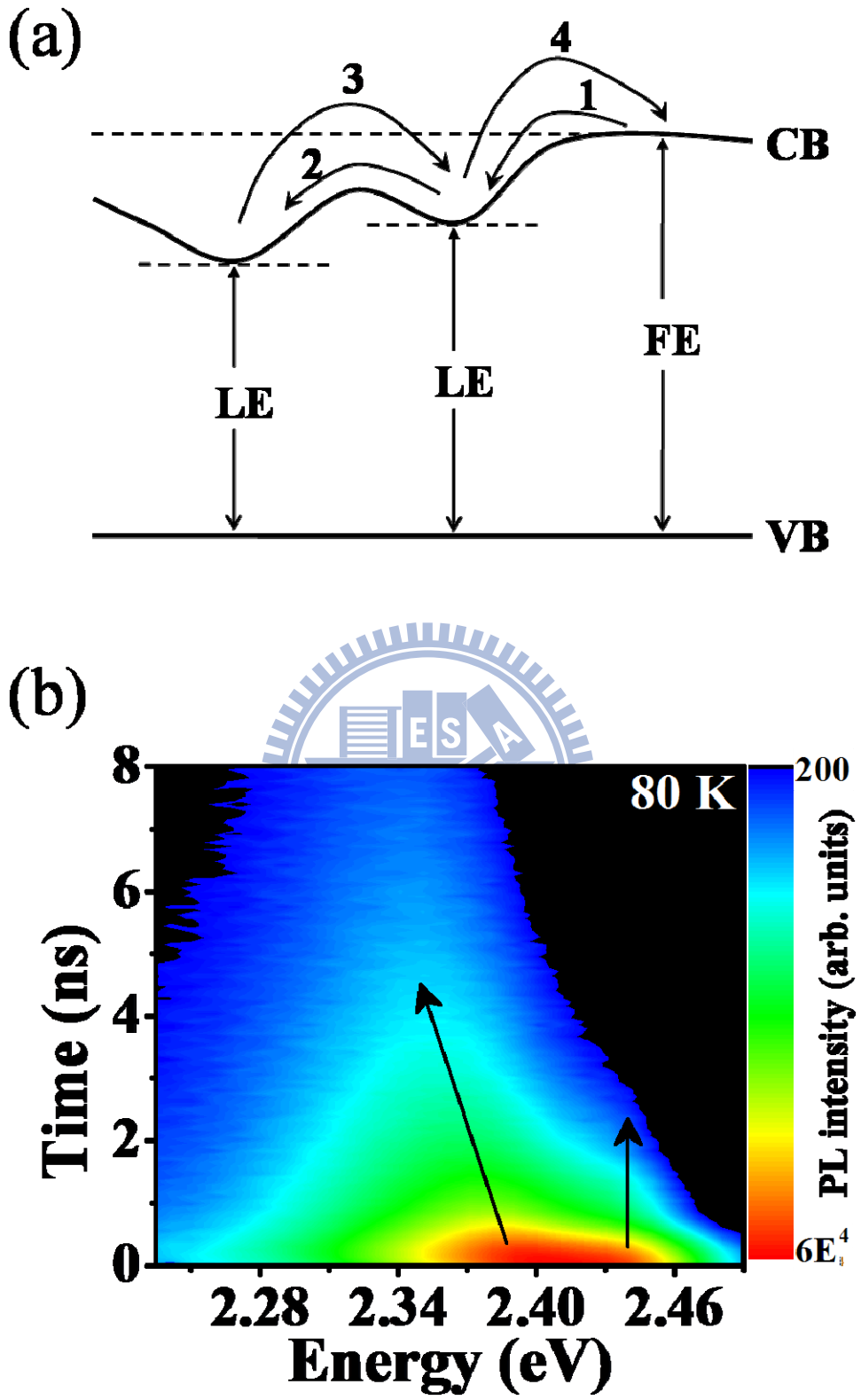

Fig. 3.12. (a) Schematic diagram used in the discussion, indicating complex relaxation channels. For simplicity only two trap states are considered. (b) TRPL image of $ZnSe_{0.947}O_{0.053}$ at 80 K.

Chapter 4 Conclusions

In summary, this study investigated carrier dynamics in $ZnSe_{1-x}O_x$ by using PL and TRPL spectroscopy. The PL peaks exhibit an S-shaped energy shift with increasing temperature. The emission is dominated by FE at high temperature while the emission is LE dominant at low temperature. Complex recombination routes induced by isoelectronic O traps are well fitted using Kohlrausch law and clarified by temperature-dependent measurements. The deduced stretching exponent β initially decreases to a minimum at 70 K. It reflects that the recombination with the electrons captured by isoelectronic O traps is significant at low temperatures. However, at higher temperatures the recombination is dominated by the free electrons thermally delocalized from the traps. Thus, the recombination from the traps gradually quenches, and then the β increases.

References

[1] J. N. Baillargeon, K. Y. Cheng, G. E. Hofler, P. J. Pearah, and K. C. Hsieh, Appl. Phys. Lett. **60**, 2540 (1992)

[2] P. J. Klar, H. Gruning, W. Heimbrodt, J. Koch, F. Hohnsdorf, W. Stolz, P. M. A. Vicente, J. Camassel, Appl. Phys. Lett. **76**, 3439 (2000)

[3] A. Polimeni, M. Capizzi, M. Geddo, M. Fischer, M. Reinhardt, and A. Forchel, Phys. Rev. B **63**, 195320 (2001)

[4] G. Y. Rudko, I. A. Buyanova, W. M. Chen, H. P. Xin, and C. W. Tu, Appl. Phys. Lett. **81**, 3984 (2002)

[5] W. Shan, W. Walukiewicz, J. W. Ager III, E. E. Haller, J. F. Geisz, D. J. Friedman, J. M. Olson, and S. R. Kurtz, Phys. Rev. Lett. **82**, 1221 (1999)

[6] W. Shan, W. Walukiewicz, K. M. Yu, J. W. Ager III, E. E. Haller, J. F. Geisz, D. J. Friedman, J. M. Olson, S. R. Kurtz, and C. Nauka, Phys. Rev. B **62**, 4211 (2000)

[7] C. Skierbiszewski, P. Perlin, P. Wisniewski, W. Knap, T. Suski, W. Walukiewicz, W. Shan, K. M. Yu, J. W. Ager, E. E. Haller, J. F. Geisz, and J. M. Olson, Appl. Phys. Lett. **76**, 2409 (2000)

[8] I. Suemune, K. Uesugi, and W. Walukiewicz, Appl. Phys. Lett. **77**, 3021 (2000)

[9] J. Wu, W. Walukiewicz, K. M. Yu, J. W. Ager, E. E. Haller, Y. G. Hong, H. P. Xin,

and C. W. Tu, Phys. Rev. B **65**, 241303 (2002).

[10] H. P. Xin, C. W. Tu, Y. Zhang, and A. Mascarenhas, Appl. Phys. Lett. **76**, 1267 (2000)

[11] K. Akimoto, T. Miyajima, and Y. Mori, Phys. Rev. B **39**, 3138 (1989)

[12] Y. Nabetani, T. Mukawa, Y. Ito, T. Kato, and T. Matsumoto, Appl. Phys. Lett. **83**, 1148 (2003)

[13] K. Iwata, P. Fons, A. Yamada, H. Shibata, K. Matsubara, K. Nakahara, H. Takasu, and S. Niki, Phys. Status Solidi B-Basic Res. **229**, 887 (2002)

[14] A. Lindsay, E. P. O'Reilly, Solid State Commun. **112**, 443 (1999)

[15] W. Walukiewicz, W. Shan, J. W. Ager III, D. R. Chamberlin, E. E. Haller, J. F. Geisz, D. J. Friedman, J. M. Olson, and S. R. Kurtz, Proceedings of the 195th Electrochemical Society Meeting, Seattle, WA (The Electrochemical Soc. Inc., Pennington, NJ, 1999), Vol. 99-11, p. 190

[16] W. Shan, W. Walukiewicz, J. W. Ager III, K. M. Yu, J. Wu, E. E. Haller, Y. Nabetani, T. Mukawa, Y. Ito, and T. Matsumoto, Appl. Phys. Lett. **83**, 299 (2003)

[17] A. Polimeni, M. Capizzi, Y. Nabetani, Y. Ito, T. Okuno, T. Kato, T. Matsumoto, and T. Hirai, Appl. Phys. Lett. **84**, 3304 (2004)

[18] Y. C. Lin, W. C. Chou, W. C. Fan, J. T. Ku, F. K. Ke, W. J. Wang, S. L. Yang, W. K. Chen, W. H. Chang, and C. H. Chia, Appl. Phys. Lett. **93**, 241909 (2008)

[19] R. Kohlrausch, Ann Phys. (Leipzig) **12**, 393 (1847)

[20] J. Jackle, Philos. Mag. B-Phys. Condens. Matter Stat. Mech. Electron. Opt. Magn. Prop. **56**, 113 (1987)

[21] H. X. Jiang, and J. Y. Lin, Phys. Rev. Lett. **64**, 2547 (1990)

[22] J. Kakalios, R. A. Street, and W. B. Jackson, Phys. Rev. Lett. **59**, 1037 (1987)

[23] H. J. Queisser, Phys. Rev. Lett. **54**, 234 (1985)

[24] R. A. Street, Advances in Physic **25**, 397 (1976)

[25] T. Hattori, H. Yugami, and M. Ishigame, Solid State Ion. **70**, 471 (1994)

[26] J. C. Phillips, Rep. Prog. Phys. **59**, 1133 (1996)

[27] G. Schlegel, J. Bohnenberger, I. Potapova, and A. Mews, Phys. Rev. Lett. **88**, 137401 (2002)

[28] B. Sturman, E. Podivilov, M. Gorkunov, Phys. Rev. Lett. **91**, 176602 (2003)

[29] C. Y. Chen, J. I. Chyi, C. K. Chao, and C. H. Wu, Electron. Lett. **45**, 1267 (2009)